Highway contributions to reactive nitrogen deposition: tracing the fate of vehicular NO_x using stable isotopes and plant biomonitors

Katherine Redling · Emily Elliott · Daniel Bain · John Sherwell

Abstract While epidemiologists have long acknowledged that automobile emissions create corridors of increased NO_x concentrations near highways, the influence of these emissions on dry nitrogen (N) deposition and effects on surrounding ecosystems are not well-characterized. This study used stable isotopes in plant tissue and dry N deposition to examine the extent of N deposition from automobile emissions along a roadside transect spanning 400 m perpendicular to a moderately trafficked highway (33,000 vehicles per day). Passive samplers were deployed monthly for four months at six stations to collect dry deposition of nitric acid (HNO_3) and nitrogen dioxide (NO_2), analyzed for concentration and natural abundance isotopic composition ($\delta^{15}N$). *Agrostis perennans* (bentgrass) and *Panicum virgatum* (switchgrass) were deployed as biomonitors to examine relative sources of N to plant tissue. Both NO_2 flux and $\delta^{15}N$–NO_2 values were significantly higher close to the road indicating a high proportion of automobile-sourced N is deposited near-road. Further, this near-road deposition occurred primarily as NO_2 prior to oxidation to HNO_3, as HNO_3 fluxes were an order of magnitude lower than NO_2 fluxes and were highest midway through the transect. Plant tissue $\delta^{15}N$ values were higher near the road, signifying the influence of automobile emissions on plant tissue composition. Importantly, N flux near the road was four times higher than background N flux measured at the nearest regional dry deposition monitoring locations. We extrapolated these results to demonstrate that the observed spatial patterns of concentrated N deposition impact our understanding of regional N deposition to watersheds when applied to a metropolitan area.

K. Redling (✉) · E. Elliott · D. Bain
Geology & Planetary Science, University of Pittsburgh, 4107 O'Hara St., Pittsburgh, PA 15260, USA
e-mail: kmm98@pitt.edu

E. Elliott
e-mail: eelliott@pitt.edu

D. Bain
e-mail: dbain@pitt.edu

J. Sherwell
MD Department of Natural Resources, Power Plant Research Program, Tawes Building B-3, Annapolis, MD 21401, USA
e-mail: jsherwell@dnr.state.md.us

Introduction

NO_x emissions from vehicular sources can create corridors of increased air pollution near highways. For example, studies document elevated atmospheric NO_x concentrations within hundreds of meters of roadways (Gilbert et al. 2007; Singer et al. 2004). However, there is limited understanding of the effects of these

emissions on the surrounding environment. Because vehicle emissions comprise $\sim$50 % of Eastern U.S. NO_x emissions (Butler et al. 2005), it is critical to identify their fate and impact on near-road ecosystems. Atmospheric reactive N compounds (including NO_x, HNO_3, and NH_3) have relatively short atmospheric lifetimes (1–8 days) and high deposition velocities, leading to near-source deposition (Kirchner et al. 2005; Moomaw 2002). Unlike emissions from regional air pollution sources (e.g., smoke stacks), dry deposition from vehicles can deposit 10s to 100s of meters from roadways (Cape et al. 2004; Kirchner et al. 2005). This spatial pattern of concentrated N deposition has implications for near-road environments, including adverse effects on plant communities. For example, studies document defoliation and changes in community structure due to N pollution near roadways (Angold 1997; Bignal et al. 2007). Furthermore, storm water infrastructure can channel near-road deposition into surface water.

Most national pollution monitoring facilities in the U.S. [such as the National Atmospheric Deposition Program and Clean Air Status and Trends Network (CASTNET)] are intentionally located in rural areas, far from major pollution sources and transportation corridors, in order to monitor regional air pollution trends. While this provides long-term assessment of background N deposition levels, the remote location of these sites likely underestimates total N deposition to the landscape. Because dry N deposition from automobiles can deposit locally, wet and dry N deposition monitored at these sites may not take into account automobile pollution (Elliott et al. 2009, 2007). Previous research suggests that N deposition observed by these networks reflects NO_y derived primarily from stationary sources rather than mobile sources (Elliott et al. 2009, 2007). Furthermore, neither monitoring network measures atmospheric NO_2 and NO_x concentrations (though they measure particulate NO_3^-, HNO_3 and, at some sites, NH_3). As a result, existing monitoring networks may underestimate NO_y and total N deposition, especially near roadways and, consequently, urban areas.

Stable isotopes of nitrogen can indicate dominant sources of NO_x emissions to precipitation and dry deposition (Elliott et al. 2009, 2007; Hastings et al. 2003). Major atmospheric NO_x sources have distinct isotopic signatures, allowing differentiation of emissions contributing to gaseous reactive N and resulting wet and dry deposition. For example, coal-fired power plant combustion generates NO_x emissions with $\delta^{15}N$ values of +10 to +20 ‰ (Felix et al. 2012; Heaton 1990). In contrast, automobile NO_x is characterized by lower $\delta^{15}N$ values, ranging from −13 to −2 ‰ for idling vehicles (Heaton 1990) and +3.7 to +9 ‰ for vehicles under high load (Ammann et al. 1999; Moore 1977). In comparison, biogenic soil NO emissions, emitted as a byproduct during nitrification and denitrification reactions, have lower $\delta^{15}N$ values relative to fossil fuel NO_x sources. Reported biogenic $\delta^{15}N$–NO values range from −49 to −19 ‰ for fertilized soils sampled during a 13-day laboratory study (Li and Wang 2008) and −27 ‰ from fertilized soils in a conventionally managed cornfield integrated over a month-long collection period (Felix and Elliott 2013).

While it is generally assumed that plants assimilate N through roots, atmospheric NO_x, HNO_3 and NH_3 taken up through the stomata can also be an important nutrient source (Garten 1993; Padgett et al. 2009; Thoene et al. 1991; Wellburn 1990). This is evidenced by studies that document similarities between $\delta^{15}N$ values in plant tissue and $\delta^{15}N$ of atmospheric NO_y across regions (Gebauer and Schulze 1991; Högberg 1997; Jung et al. 1997) and near roads (Ammann et al. 1999; Pearson et al. 2000; Saurer et al. 2004).

This study examined the extent of N loading along a transect perpendicular to a moderately trafficked highway ($\sim$33,000 vehicles per day) using passive sampling of dry reactive N fluxes and $\delta^{15}N$ values. In addition, the effects of increased roadway N deposition on local vegetation were explored using the isotopic composition of plant tissue as a biomonitor of atmospheric N exposure. By coupling plant tissue natural abundance isotopic composition with concentration and natural abundance isotopic composition of atmospheric reactive N, we assessed the extent of N transport in near-road environments, the fate of this reactive N, and the potential influence on local vegetation.

Methods

Site description

The road transect was located at the Carnegie Museum of Natural History Powdermill Nature Reserve near Donegal, Pennsylvania (USA) (N 40°07′42.2″;

W 79°17′11.7″). The transect was situated in a meadow that abuts Interstate-76, a five-lane highway that conveys an annual average of $\sim 33{,}300$ vehicles per day (2008 data) (Pennsylvania_Department_of_Transportation 2009) (Fig. 1). This is similar to daily traffic density in a moderate-sized city but is lower than larger metropolitan areas. For example, I-376 in Pittsburgh, Pennsylvania has an annual average daily traffic of 31,000 vehicles per day, whereas traffic volume on I-276 in Philadelphia, Pennsylvania is 105,000 vehicles per day (Pennsylvania_Department_of_Transportation 2009). While multiple transects are preferable, logistical constraints including both land owner access and available funding limited this study to a single transect.

Sampling stations were established at 2, 12, 30, 90, 188 and 460 m along the transect from the roadway (Fig. 1). Sampling sites were selected based on accessibility and were located closer together near

the road to capture the exponential decline in NO_2 flux expected near the road. The 460 m length of the gradient was based on the maximum length to the edge of the field, which was adjacent to a forest. While previous studies had control sites 1,000 meters from the road (Ammann et al. 1999; Saurer et al. 2004), this was not possible in our transect location due to vegetation change from meadow to forest. We used 460 m as our control site because previous literature demonstrated that 90 % of NH_3 and NO_2 deposition occurs within 15 m of the road (Cape et al. 2004). The transect was located in a rural area, far from point sources of NO_x emissions. In this isolated roadside environment, the dominant sources of NO_2 and HNO_3 were expected to be soil biogenic and vehicle NO_x emissions.

Plant sampling and analysis

Each station contained two 7.5 liter pots, one *Agrostis perennans* (bentgrass) and one *Panicum virgatum* (switchgrass), with approximately fifty individual grass plants per pot. Bentgrass and switchgrass were chosen because they are drought-resistant natives with C-3 and C-4 photosynthetic pathways, respectively. The 12 m station contained two switchgrass; it did not contain bentgrass due to plant mortality at that station. No plants were sited at 2 m due to highway right-of-way restrictions. Potted plants were used rather than native vegetation to control natural variability in soil N content, soil type, specimen age, and species along the transect. All plants along the transect were grown from seed in the same indoor greenhouse, ensuring that all plants would start with similar isotopic compositions. Likewise, all the plants were grown and eventually re-potted in well-homogenized potting soil, ensuring limited isotopic variability between soil N in each pot. Pots were doubled to prevent water loss, intrusion of native soil and root growth through the bottom of the pots. Pots were placed in holes in the ground to further prevent water loss. By controlling the soil media, using multiple individuals and effectively restricting the plants to their pots, the amount of isotopic variability between individual plants prior to exposure was limited. Because plant roots could not access soil beyond the pot exterior, it was assumed that plants only received nutrients from the soil in the pot and atmospheric deposition. Plants were watered upon

Fig. 1 Aerial photograph of road transect with sampling stations labeled. R1–R6 correspond with 2, 12, 30, 90, 188 and 460 m stations, respectively

initial deployment with local tap water, but for the remainder of the study received only precipitation. While nitrate and ammonium are present in Western Pennsylvania precipitation and would act as a plant nutrient, it is expected that across such a small spatial scale, isotopic variability in rain water nitrate and ammonium $\delta^{15}N$ values between the sites would be minimal. With these experimental controls on isotopic composition in place, as the plants gained biomass throughout the summer, the biomass acquired the isotopic signature of the CO_2 from the surrounding air and reactive N from either stomatal uptake of gaseous reactive N or root uptake of dry deposited reactive N or potting soil N.

Plants and soils were sampled monthly from July through October, 2008. Samples were cut with scissors, washed with 18 MΩ water to remove any dry deposition and dirt from the leaves and placed in individual bags. Grass samples from each pot were composited into a single sample, containing leaves from the entire population of plants in the pot. Grasses were not completely harvested—approximately 50 g of leaves were cut monthly. Approximately 100 g of potting soil were spooned out of the pots from a depth of 2–5 cm and placed in individual bags. All samples were transported on ice to laboratories at the University of Pittsburgh and stored frozen to prevent tissue breakdown. Samples were subsequently freeze-dried and ground with a coffee grinder and mortar and pestle and packed into tin capsules for isotopic analysis. Isotopic analysis was conducted using a EuroVector high temperature elemental analyzer connected to a GV Instruments Isoprime Continuous Flow Isotope Ratio Mass Spectrometer (CF-IRMS) at the Regional Stable Isotope Laboratory for Earth and Environmental Science at the University of Pittsburgh. Precisions were <0.1 ‰ for $\delta^{13}C$ and $\delta^{15}N$ on duplicate samples. All populations are treated as normally distributed and potential correlations were evaluated using linear regressions.

Dry deposition sampling and analysis

NO_2 and HNO_3 were collected using passive diffusion samplers that collect individual N compounds on a chemically reactive filter pad. This is an effective and inexpensive method for monitoring dry deposition (Bytnerowicz et al. 2005; Golden et al. 2008) and isotopic composition (Elliott et al. 2009) of N

compounds. For NO_2, 14.5 mm TEA-coated filters and samplers (Ogawa, USA) were used that contained two filters held in place by a diffusion barrier and stainless steel screens. HNO_3 was collected using 47 mm nylon filters (Pall Corporation) coupled with a Zefluor^{TM} PTFE membrane (Pall Corporation) in a PVC housing where each sampler assembly contained one HNO_3 filter (Bytnerowicz et al. 2005). We deployed two filter pads, one for isotopic analysis and one for concentration measurements, for both NO_2 and HNO_3 at each site for one month intervals. This length of time ensured sufficient material was collected to perform both concentration measurements and isotopic analysis. Filters were changed in the field each month concurrent with grass and soil sampling. Exposed filters were loaded into centrifuge tubes and frozen until analysis. Field and laboratory blanks were used to determine background levels of deposition on the filters prior to deployment. Missing data points included the 2 and 12 m stations in July (NO_2 and HNO_3) and the 30 m station in August (NO_2) due to highway right-of-way restrictions and vandalism, respectively.

For concentration measurements of NO_2 and HNO_3, each filter was eluted with 5 mL of 18 MΩ water to produce NO_2^- and NO_3^-. Eluant concentrations were analyzed on a Dionex ICS2000 Ion Chromatograph. For isotopic analysis of NO_2 and HNO_3, the second filter of each sample was eluted in 5 mL of 18 MΩ water. The bacterial denitrification method was used to convert eluted nitrite and nitrate into 10 nmol of N_2O gas (Casciotti et al. 2002; Sigman et al. 2001). The resulting gas was introduced into a GV Instruments Isoprime CF-IRMS. Precisions were <0.25 ‰ for $\delta^{15}N$ on duplicate analyses. Samples with <0.23 mg L^{-1} eluant concentrations were not analyzed due to insufficient sample mass. This included four NO_2 samples: the 188 and 460 m stations from July and the 90 and 188 m stations from August.

While it is challenging to directly measure dry deposition and associated deposition velocities, concentrations on passive samplers were used to estimate N flux. In this study, we estimated flux using two methods. For the first estimate, we used the method described by Golden et al. (2008), hereafter referred to as the "Golden method" in which

$$F = (c \times v)/(a \times d) \qquad (1)$$

where F is flux, c is concentration measured in filter eluant, v is elution volume, a is the effective filter area and d is number of days the filter was exposed. For the second estimate, we used a method described by Roadman et al. (2003), hereafter referred to as the "Roadman method" in which

$$C = (m/t)/M \tag{2}$$

$$F = C \times V_d \tag{3}$$

where C is average ambient concentration, m is mass of N on the filter, t is time the filter was exposed, M is the mass transfer coefficient, F is flux and V_d is deposition velocity. For Roadman method calculations, mass transfer coefficients derived from the literature were used for each type of sampler design. For the NO_2 sampler design, there were two mass transfer coefficients reported, 12.1 cm^3 min^{-1} (Tang et al. 2001) and 9.5 cm^3 min^{-1} (Yu et al. 2008), hereafter referred to as the "Roadman low" and "Roadman high" scenarios, respectively. To our knowledge, only one mass transfer coefficient has been reported for the HNO_3 sampler used in this study [31.855 m^3 h^{-1} (Bytnerowicz et al. 2005)]. As such, only one flux was calculated using the "Roadman method" for HNO_3.

Deposition velocities for NO_2 and HNO_3 were estimated for the road transect using CALPUFF (US Environmental Protection Agency 2009). CALPUFF is a Lagrangian puff dispersion model that simulates effects of spatial and temporal variations in meteorological data on dispersion, transport, and deposition of pollutant species. Continuous emissions from air pollution sources, such as mobile sources, are simulated by a series of puffs tracked during downwind transport. CALPUFF estimates dry deposition velocity as a function of land use at the location of each puff.

CALPUFF-derived deposition velocities for NO_2 spanned a range (0.0018 and 0.001 m s^{-1}); this range falls within literature-reported values for NO_2 (0.001 m s^{-1}) (Hauglustaine et al. 1994). Estimated deposition velocities for HNO_3 derived from CALPUFF were 0.0035 m s^{-1}. While this value is lower than literature-reported values (0.04 m s^{-1} for average continental deposition (Hauglustaine et al. 1994) and 0.008–0.033 m s^{-1} modeled for various land types (Clarke et al. 1997), it reflects the highly variable deposition velocities for HNO_3 and using lower values is a more conservative approach in the flux calculations.

For this study, this range in deposition velocities was combined with the range of reported mass transfer coefficients to yield scenarios representing both the highest and lowest potential fluxes for the "Roadman high" and "Roadman low" scenarios, respectively.

Filter concentrations reflected monthly average concentrations for each month of the study. For accuracy, spatial and temporal variations in NO_2 and HNO_3 (Fig. 3) were reported as monthly fluxes (kg ha^{-1} $month^{-1}$). However, we also extrapolated average NO_2 and HNO_3 flux calculations (Fig. 2) for an entire year period and report annual fluxes (kg ha^{-1} $year^{-1}$) to facilitate conservative comparisons with other monitoring studies using the kg ha^{-1} $year^{-1}$ convention. All fluxes were reported as NO_2–N or HNO_3–N.

Results

Reactive N fluxes

Concentrations for NO_2 ranged from below detection to 6.4 ppb, corresponding to an average NO_2 flux for all months ranging from 0.9 to 4.2 kg ha^{-1} $year^{-1}$ for the Roadman high estimate, 0.4 to 1.3 kg ha^{-1} $year^{-1}$ for the Roadman low estimate and 0.5 to 2.2 kg ha^{-1} $year^{-1}$ for the Golden estimate (Fig. 2a). Highest average fluxes occurred at the 2 m station. NO_2 fluxes decreased exponentially with distance from the road with the lowest fluxes generally observed at the 460 m station. NO_2 flux varied temporally (Fig. 3a). Throughout 5 months of observations, the spatial gradient in NO_2 flux was present in all months, but with varying intensity. In August NO_2 flux was three times higher at the station 2 m from the road than at the 460 m station. In September, October and November roadside NO_2 flux was 2.6, 4 and 4.4 times higher than the 460 m station, respectively. The highest estimated flux throughout the study occurred in October at the 2 m station (0.5, 0.3 and 0.2 kg ha^{-1} $month^{-1}$ with the Roadman high, Golden and Roadman low estimates, respectively).

HNO_3 flux exhibited spatial and temporal patterns distinct from NO_2 flux patterns. HNO_3 flux was an order of magnitude lower than NO_2, with average flux for all months ranging from 0.13 to 0.26 kg ha^{-1} $year^{-1}$ for the Golden method and 0.06 to 0.10 kg ha^{-1} $year^{-1}$ for

Fig. 2 N flux, atmospheric N isotopes, plant isotopes and C:N ratios, and soil N isotopes. For NO_2 and HNO_3 flux, squares are Golden method estimates, triangles are Roadman low estimates and diamonds are Roadman high estimates. Plant data does not include July; as the plants acquired biomass, the N isotopes changed as juvenile plants matured. July data was a mix between seedling values from June and mature plants in August. Plots c-l are *box and whisker plots*, in which the *box* represents the upper and lower quartile and the *whiskers* represent the minimum and maximum data point. The *center line* in the box is the median value. Outliers are shown as *black dots* with *lines* through them
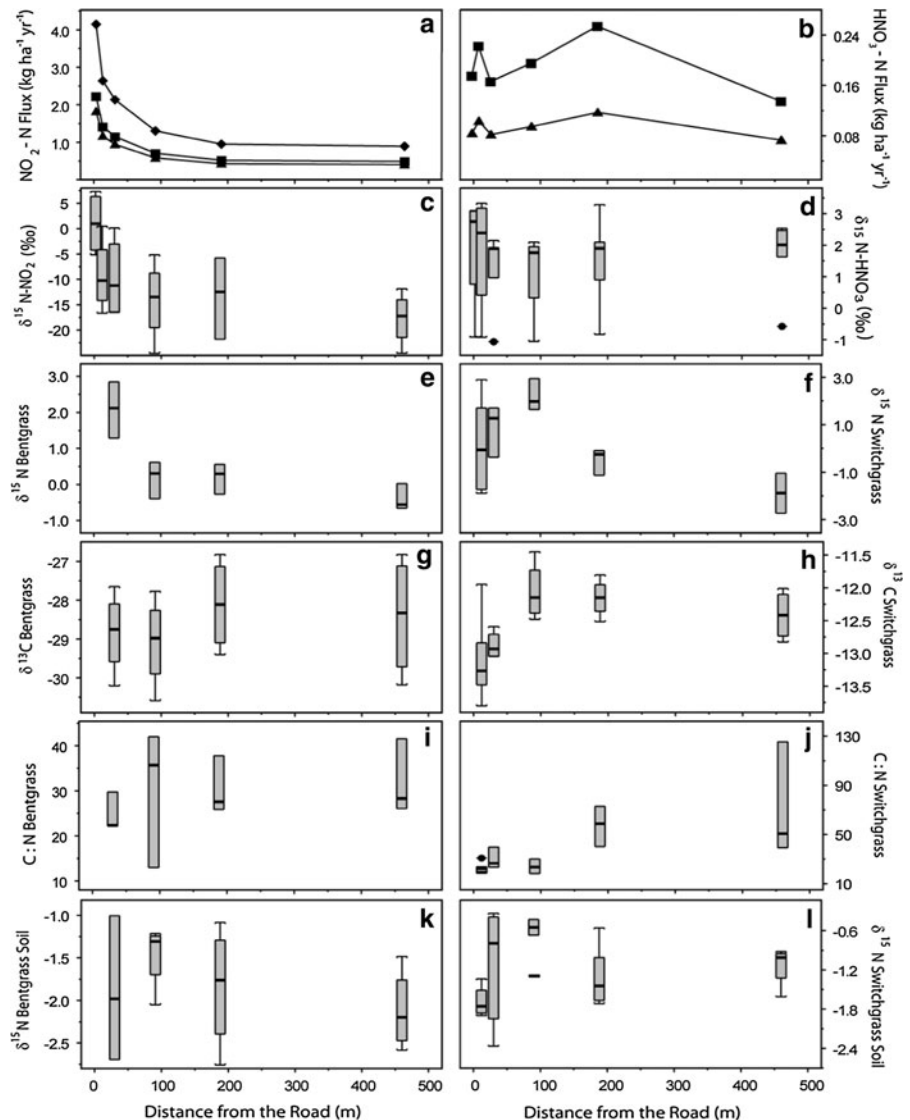
the Roadman method (Fig. 2b). HNO_3 flux peaked at two transect stations (12 and 188 m) and was generally highest in October and November.

Isotopic composition of dry deposition

$\delta^{15}N$–NO_2 followed a spatial pattern similar to NO_2 flux; mean $\delta^{15}N$ values decreased with distance from the road (Fig. 2c). The 2 m station had values ranging from −5.1 to +7.3 ‰. The 460 m station had values ranging from −11.9 to −24.6 ‰. Values at these two stations were significantly different (ANOVA, $p = 0.02$).

Additionally, $\delta^{15}N$–NO_2 exhibited seasonal variation similar to seasonal variations in NO_2 flux

(Fig. 3c). $\delta^{15}N$–NO_2 was lowest during September at most stations (12, 90, 188 and 460 m). During October and November $\delta^{15}N$–NO_2 increased at all stations. The highest values were in November, during periods of highest NO_2 flux.

In comparison, $\delta^{15}N$–HNO_3 did not exhibit a defined spatial gradient (Fig. 2d). $\delta^{15}N$–HNO_3 values ranged from −1.1 to +3.3 ‰, which was within the vehicle $\delta^{15}N$–NO_x range; however, individual stations were not significantly different each other (ANOVA, $p = 0.05$). Temporal trends in $\delta^{15}N$–HNO_3 were dominated by lower $\delta^{15}N$ values at all stations in September relative to other months (Fig. 3d). However, relative to NO_2, $\delta^{15}N$–HNO_3 values spanned a

Fig. 3 Monthly variations in N flux (in kg ha^{-1} month^{-1}), atmospheric N isotopes, plant tissue isotope, and plant tissue C:N ratios at each station. For NO$_2$ and HNO$_3$ flux, *squares* are Golden method estimates, *triangles* are Roadman low estimates, and *diamonds* are Roadman high estimates. For atmospheric N isotopes, missing values (due to low concentrations) are omitted. For plant tissue plots, neither grass was placed at the 2 m station. For switchgrass plots, the 12 m station had two pots of grass; all other stations had one pot. There were no bentgrass pots at the 12 m station
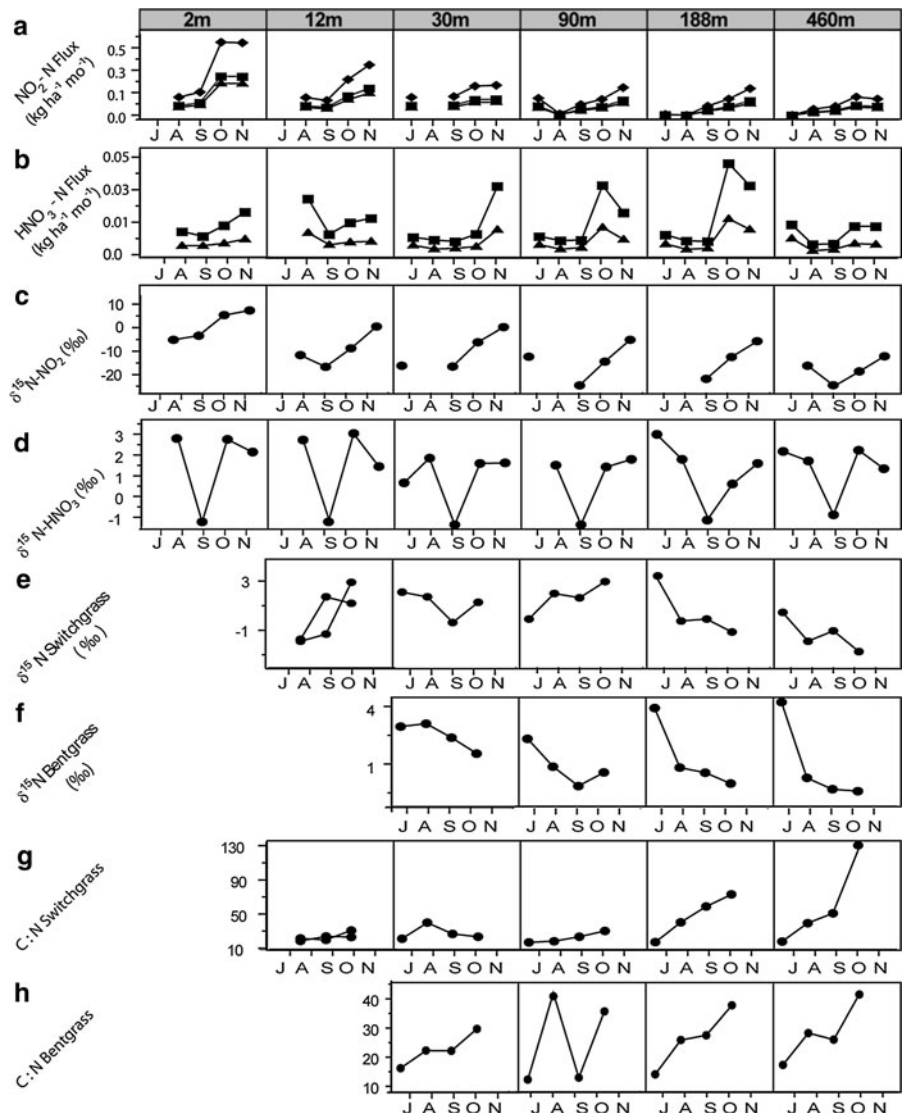
smaller range and, apart from September values, were relatively constant across the stations during the study period.

Plant tissue and soils

We observed pronounced spatial gradients in δ^{15}N values of bentgrass and switchgrass tissue (Fig. 2e, f). Bentgrass δ^{15}N values were highest closest to the road and were significantly correlated with distance from the road (linear regression, $R^2 = 0.69$, $p < 0.001$). Bentgrass δ^{15}N values at the 30 m station were significantly different from those at stations at 90,

188 and 460 m (ANOVA, $p = 0.02$). Switchgrass δ^{15}N values were more spatially variable. Switchgrass δ^{15}N values were not correlated with distance from the road, likely because the peak mean value was 90 m from the roadway (Fig. 2f). Switchgrass δ^{15}N values at 12 m were the most variable of all the stations; however average δ^{15}N values at 12 m were higher than those at 460 m. The only significant difference between average δ^{15}N values at all the stations was between 90 and 460 m stations (ANOVA, $p = 0.03$). Temporally, δ^{15}N-bentgrass decreased slightly from August until October at all stations (Fig. 3f). In comparison, temporal changes in switchgrass δ^{15}N varied by station (Fig. 3e); at the 12 and 30 m stations,

$\delta^{15}N$ increased throughout the months of the study, whereas at all other stations $\delta^{15}N$ decreased.

Soil $\delta^{15}N$ from switchgrass pots varied most at the 12 and 30 m sites, with $\delta^{15}N$ values peaking at the 90 m station and decreasing with distance from the road, consistent with $\delta^{15}N$ values of switchgrass tissue (Fig. 2l). In contrast, $\delta^{15}N$ of bentgrass soil (Fig. 2k) showed no clear trends across the transect and was dissimilar to bentgrass tissue $\delta^{15}N$.

C:N in switchgrass tissue was lowest closest to the road and increased and became more variable with distance from the road (linear regression, $R^2 = 0.43$, $p < 0.003$) (Fig. 2j). Bentgrass C:N also increased with distance from the road; however, this relationship was not significant (Fig. 2i). Temporally, while initial switchgrass C:N values were similar at all stations, throughout the months of the study, C:N increased at the 188 and 460 m station (Fig. 3g). In August, September and October, C:N ratios at the 12 m station were significantly different from those at 460 m (ANOVA, $p = 0.05$). Bentgrass exhibited a similar temporal response. Bentgrass C:N was comparable at all stations in July (Fig. 3h); however by August, C:N ratios were higher at the 460 m station relative to those stations closer to the road.

Bentgrass $\delta^{13}C$ values were more positive farther from the road (Fig. 2g). However, this relationship was not significant and varied by month. Temporally, in July and August, bentgrass $\delta^{13}C$ values were approximately the same across the entire transect. However, in September and October, the 460 m station had $\delta^{13}C$ values approximately 1 ‰ higher than the 30 m station. Switchgrass $\delta^{13}C$ values were correlated with distance from the road (linear regression, $R^2 = 0.28$, $p < 0.03$) (Fig. 2h). Switchgrass $\delta^{13}C$ values at 12 m were significantly lower than at 90 and 188 m (ANOVA, $p = 0.05$). In each month, the 460 m station had values ~ 1 ‰ higher than the 12 m station.

Discussion

Patterns in near-road reactive N fluxes and comparison to CASTNET deposition monitoring

The spatial pattern of rapid decreases in NO_2 fluxes with distance from the road observed in this study was consistent with studies that document elevated concentrations and flux of NO_2 near roadways (Cape et al. 2004; Kirchner et al. 2005). Temporal increases in NO_2 fluxes during October and November were also consistent with studies documenting increases in NO_2 flux during colder months (Atkins and Lee 1998; Kirby et al. 1998). Higher NO_2 fluxes during colder months were attributable to higher stationary source NO_x emissions during colder months (Elliott et al. 2009), seasonal changes in oxidation pathways, or decreased NO_2 uptake by stomata at the end of the growing season (Hargreaves et al. 1992).

As an oxidation product of NO_2, HNO_3 is formed at a greater distance from the road and thus accounts for more complicated spatial patterns in HNO_3 fluxes. In addition, HNO_3 has highly variable deposition velocities, and can more readily deposit on surfaces than NO_2. The variations in deposition velocity may have accounted for complex spatial patterns in HNO_3 flux, but were not captured by the flux calculations, which use a single deposition velocity.

Comparison of total N flux near the roadway with background levels of N deposition measured at a local CASTNET site revealed an underestimation of N deposition reaching the landscape by regional monitoring networks. Total dry deposition measured at the nearest CASTNET site (Laurel Hill LRL 117, which is 16 km from the road transect) in 2008 was 1.04 kg ha^{-1} year^{-1}. This included measurements of particulate nitrate, dry NH_4, and HNO_3 (U.S._EPA_CASTNET 2008). In comparison, at the 2 m road transect station, the total annual deposition was estimated to be 1.9, 2.4 and 4.2 kg ha^{-1} year^{-1} for total N (NO_2 plus HNO_3), using the Roadman low, Golden and Roadman high methods of estimation, respectively. This deposition was based on the average of monthly observed data for the 4 months of the study. Although this estimate was based on a partial year of data, it was expected that this was a conservative estimate due to higher NO_2 concentrations expected during winter months. There were no significant changes in NO_2 flux and $\delta^{15}N$ between the 90 and 460 m sites, indicating that by 460 m a background level was reached. At the 460 m station, which was most likely reflective of background regional dry N deposition, total N flux was estimated at 0.4, 0.6 and 0.9 kg ha^{-1} year^{-1} with the Roadman low, Golden and Roadman high methods, respectively. Of the three estimates, the Roadman high

estimate at this station (0.93 kg ha^{-1} year^{-1}) was most similar to flux measured at the CASTNET site (1.04 kg ha^{-1} year^{-1}); therefore we used the Roadman high method to compare flux along the rest of the transect (Fig. 4). This comparison indicated an additional 3.3 kg ha^{-1} year^{-1} above ambient background NO_2 and HNO_3 fluxes were deposited within 2 m of the roadway; this was 4 times higher than the CASTNET site (Fig. 4). At the 12 m station, the Roadman high estimate was 2.7 kg ha^{-1} year^{-1}, which was an additional 1.8 kg ha^{-1} year^{-1} above background (2.6 times higher than CASTNET). These results illustrate that increased N fluxes near roadways can create continuous corridors of concentrated N deposition across the landscape. This has important implications not only for air quality, but also for water quality and ecosystem health, especially in urban areas characterized by high road densities. These findings highlight the need for longer term, spatially replicated monitoring of roadsides to more accurately characterize total N flux to the land surface.

Using NO_2 and HNO_3 isotopes to evaluate sources of dry N deposition along the road transect

Average $\delta^{15}N$–NO_2 values at the 2 m station (mean = +1.0 ± 3.5 ‰) were close to the reported vehicle range for $\delta^{15}N$–NO_x (+3.7 to +9 ‰), whereas values at all other stations indicated mixing between vehicular and biogenic NO_x sources, dependent on distance from the highway. We used a two endmember mixing model to estimate contributions of
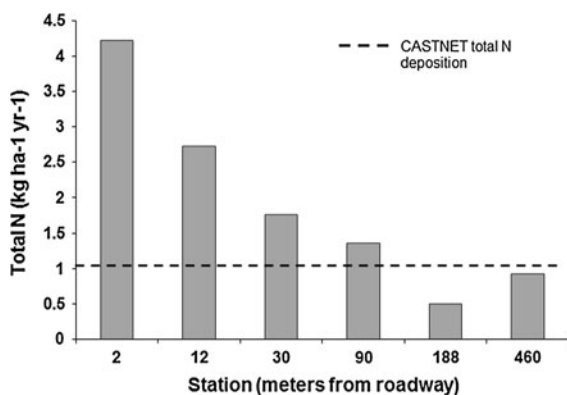

Fig. 4 Total N deposition in kg ha^{-1} year^{-1} ($NO_2 + HNO_3$) along the road gradient using the Roadman high estimate in comparison with local CASTNET site total N deposition measurements

biogenic and automobile emissions to each station along the road transect. The model assumed that biogenic and automobile NO_x were the primary sources of NO_2 along the transect and that contributions from other NO_x sources (e.g. power plants) were regionally distributed and thus affected all sites along the transect equally. The mixing model was calculated as follows:

$$\delta^{15}N_{pred} = \left(F_b \times \delta^{15}N_b\right) + \left(F_a \times \delta^{15}N_a\right) \qquad (4)$$

where $\delta^{15}N_{pred}$ is the predicted $\delta^{15}N$–NO_2 value, F_b is the fraction biogenic, $\delta^{15}N_b$ is the biogenic $\delta^{15}N$–NO_2 value, F_a is the fraction automobile, and $\delta^{15}N_a$ is the automobile $\delta^{15}N$–NO_2 value. Values for $\delta^{15}N_b$ [−19 to −49 ‰ (Li and Wang 2008)] and $\delta^{15}N_a$ [+3.7 to +9 ‰ (Ammann et al. 1999; Heaton 1990; Moore 1977)] were obtained from literature values for biogenic and automobile emissions, respectively. Two versions of the mixing model were calculated, using the widest range in reported values (−49 and +9 ‰) and the narrowest range (−19 and +3.7 ‰) for $\delta^{15}N_a$ and $\delta^{15}N_b$, respectively. Predicted values were compared to observed values to estimate the percent contributions from biogenic and automobile emissions to each station in each month. Because the endmembers of the mixing model spanned a wide range for both biogenic and automobile emissions, results from the mixing model produced large ranges in percentages for biogenic and automobile emissions at each station. Future studies that constrain the isotopic values of endmembers will improve our ability to apportion these source contributions using mixing models.

The lower $\delta^{15}N$–NO_2 values in August and September reflected the influence of biogenic sources during the growing season. According to the mixing model, at the 2 m station, in August and September, automobile sources accounted for 61–79 % of NO_2, whereas in October and November, 93–100 % of NO_2 at this station was from automobiles. Despite the seasonal variation, the spatial gradient in $\delta^{15}N$–NO_2 values remained consistent during each sampling month, indicating that mobile NO_2 emissions continually influenced the transect throughout the study, especially within 12 m of the road. In comparison, at the 460 m site in October and November between 3 and 64 % of NO_2 was from automobile sources, reflecting the dominance of biogenic emissions to ambient NO_2 concentrations.

In contrast, $\delta^{15}N$–HNO_3 did not exhibit a defined spatial gradient. This suggested that measured HNO_3 included N from multiple sources, in addition to vehicle-sourced NO_2. This was likely given the highly variable deposition velocity and longer atmospheric lifetime of HNO_3 (up to 8 days) and the potential for regional transport (Neuman et al. 2006). Temporal trends in $\delta^{15}N$–HNO_3 were dominated by lower $\delta^{15}N$ values at all stations in September relative to other months. Relative to NO_2, $\delta^{15}N$–HNO_3 values spanned a smaller range and, apart from September values, were relatively constant across the stations during the study period. However, the seasonal variation could indicate a regional fossil fuel signal; $\delta^{15}N$–HNO_3 from regional transport could indicate influence from coal-burning power plants, with higher values corresponding with increases in electricity usage for summer air conditioning in July and August and winter heating in October and November (Fig. 3d).

Effects of automobile emissions on plant tissue

The strong correlation between $\delta^{15}N$ values and distance from the road in Bentgrass indicates plants closer to the road were taking up excess N from a source with high $\delta^{15}N$ values. This could directly result from uptake of isotopically enriched dry deposition from automobile pollution (either via stomatal or root uptake). Alternatively, Bentgrass pots near the road may have been subject to accelerated rates of N cycling due to higher deposition fluxes and thus subject to additional fractionating mechanisms prior to root uptake (Dawson et al. 2002). These findings are in agreement with other studies that report increases in plant tissue $\delta^{15}N$ near roadways in comparison with control sites (Ammann et al. 1999; Pearson et al. 2000; Saurer et al. 2004). Furthermore, these variations rule out influence from regional sources, as regional emissions would likely affect all plants along the transect.

In contrast, switchgrass $\delta^{15}N$ values were not correlated with distance from the road. These results suggested that the two grass species derived differing proportions of nutrients from roots, stomatal uptake, and various reactive N compounds (e.g., NH_3, NO_2, and HNO_3). While bentgrass may have derived N nutrition from atmospheric uptake, switchgrass may have taken up more N through the roots. One potential

explanation for these differences is that, as a C3 plant, bentgrass has a higher stomatal conductance relative to C4 species (i.e., switchgrass). For example, Okano et al. (1988) observed strong correlations between NO_2 uptake and stomatal conductance of several herbaceous species.

Temporal trends in spatial patterns of $\delta^{15}N$ also suggested bentgrass may be a more robust indicator of atmospheric N uptake than switchgrass. Bentgrass $\delta^{15}N$ values were consistently higher at the site close to the road in August, September and October, perhaps indicating possible uptake from atmospheric N sources. Bentgrass $\delta^{15}N$ values decreased slightly throughout the months of the study. This was not necessarily expected given increasing N flux during those months; however, September through October marks the end of the plant growing season in this region, which is characterized by slowed growth and translocation of N from roots to shoots, which limits N uptake during this period. In contrast to the temporally consistent spatial pattern of bentgrass $\delta^{15}N$ values, switchgrass $\delta^{15}N$ varied by month without clear trends, indicating that atmospheric dry N deposition may have been a less important nutrient source. This was further reflected in soil $\delta^{15}N$ values for switchgrass and bentgrass. The similarity between switchgrass tissue and soil $\delta^{15}N$ values suggested switchgrass was primarily receiving N nutrition from the soil. In contrast, $\delta^{15}N$ of bentgrass soil showed no clear trends across the transect and was dissimilar to bentgrass tissue $\delta^{15}N$. These results suggested that bentgrass tissue may have incorporated N derived from atmospheric sources and thus may be a more robust biomonitor for atmospheric N than switchgrass. While the spatiotemporal variations in dry N deposition, plant tissue, and soil $\delta^{15}N$ values cannot conclusively determine nutrient sources, uptake pathways, or fractionation mechanisms, it is anticipated that these relationships will be the building blocks for future studies to examine these complex dynamics.

Plant tissue total N and $\delta^{15}N$ values are generally not correlated (Pearson et al. 2000), making C:N ratios in plant tissue another tool that can be used to evaluate effects of excess N deposition on plants. Both switchgrass and bentgrass C:N values increased with increasing distance from the road, indicating that plants near the road had a higher supply of N available than plants far from the road. Furthermore, the temporal variations observed in switchgrass and

bentgrass C:N ratios also indicated that plants far from the road were the most N limited; as plants used up nutrients in the potting soil at stations far from the road, the C:N ratios increased throughout the study. In contrast, plants closer to the road received a continuous supply of N deposition, which contributed to their N nutrition and resulted in lower C:N ratios. This mechanism can explain why species compositions in plant communities near roadways often have a greater proportion of N-tolerant plants (Angold 1997; Bignal et al. 2007).

C isotopes provided another approach for examining the impacts of fossil fuel emissions on plant tissue along the road transect. Because plants utilize atmospheric CO_2 during photosynthesis, C isotopes in plant tissue can indicate the sources of CO_2 to which plants were exposed. The two sources of CO_2 in this system are background atmospheric CO_2, characterized by

Fig. 5 Estimated N deposition within 12 m of roadways in Southeastern Pennsylvania. 45 % of roadways in the Philadelphia region have N deposition higher than background levels measured by CASTNET in rural Pennsylvania. On heavily-trafficked roads, deposition may be as much as 14 times higher than background
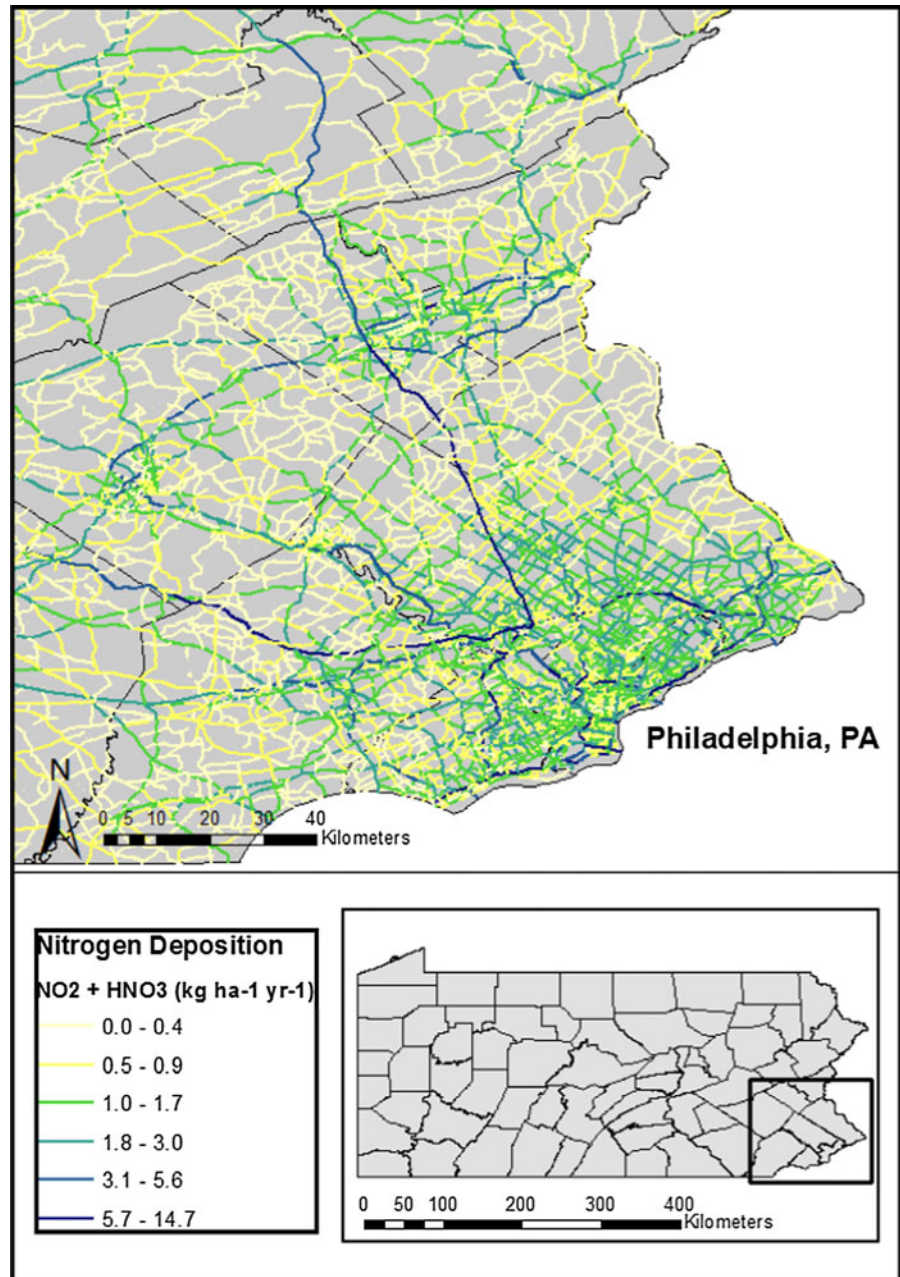
$\delta^{13}C$ of -8 ‰ (Keeling 1958), and fossil fuel CO_2 from automobiles, with a $\delta^{13}C$ value of approximately -27 ‰ (Bush et al. 2007; Clark-Thorne and Yapp 2003). Thus plants impacted by fossil fuel emissions were expected to have lower $\delta^{13}C$ values relative to plants primarily exposed to ambient CO_2. In this study, both bentgrass and switchgrass had lower $\delta^{13}C$ values at the station closest to the road. This was in agreement with another road transect study in which $\delta^{13}C$ values in plant tissue 1 m from a roadway were ~ 1 ‰ lower than 50 m from the road (Lichtfouse et al. 2002). This also agreed with a study along a longer urban to rural transect, where $\delta^{13}C$ values in plant tissue were lower at urban sites with higher fossil fuel emissions (Lichtfouse et al. 2002).

Implications for regional deposition estimates

To explore how these spatial patterns influence deposition rates in regions with greater traffic volumes, we modeled $NO_2 + HNO_3$ fluxes deposited within 12 m of Pennsylvania roads using our flux observations, 2008 traffic volume estimates, and assuming a linear relationship between traffic volume and flux (Fig. 5). The results demonstrated that 20 % of roadways in Pennsylvania likely exceeded background levels for this region measured by CASTNET (1.04 kg ha^{-1} year^{-1}); in urban Philadelphia, this figure increased to 45 % of roadways. Furthermore, while moderately trafficked roads were expected to have deposition fluxes 3–5 times background levels, up to 14 times background levels were expected in the most heavily trafficked corridors near urban Philadelphia (Fig. 5).

Conclusions

In a meadow abutting a moderately trafficked interstate highway, automobile emissions conservatively contributed four times more N deposition to near-road environments than regional background deposition. However, near-road deposition fluxes were not necessarily captured by existing national monitoring networks designed to measure regional N deposition. Further, these networks do not measure NO_2, a primary pollutant from automobiles and the dominant source of N flux in this study. Together, these results highlight the need for accurate assessment of total

atmospheric N flux to the landscape, establishment of more precise N budgets, and development of useful mitigation strategies for atmospheric N pollution, which will require characterization of deposition reaching urban and near roadway areas.

Furthermore, the results presented here suggest that near-road hotspots of increased N deposition are important, yet poorly constrained, inputs to ecosystems adjacent to and downstream of roadways. For example, while excess N may negatively impact near-road vegetation and soils, increased plant uptake of N near roadways also suggests roadside plants may potentially be used to mitigate the effects of excess N, although further research is needed to verify this. Additionally, roadside storm water infrastructure can potentially channel excess dry N deposition directly into sewers and surface water, where elevated nitrate concentrations in waters can contribute to acidification and eutrophication. This could be an underestimated source of reactive N inputs to urban watersheds where high export rates have been documented (Divers et al. 2012; Groffman et al. 2004; Hatt et al. 2004) and also to regional coastal watersheds, such as the Chesapeake Bay, that contain several metropolitan areas and experience annual hypoxia from nutrient additions.

References

Ammann M, Siegwolf R, Pichlmayer F, Suter M, Saurer M, Brunold C (1999) Estimating the uptake of traffic-derived NO_2 from ^{15}N abundance in Norway spruce needles. Oecologia 118(2):124–131

Angold PG (1997) The impact of a road upon adjacent heathland vegetation: effects on plant species composition. J Appl Ecol 34(2):409–417

Atkins DHF, Lee DS (1998) Spatial and temporal variation of rural nitrogen dioxide concentrations across the United Kingdom. Atmos Environ 29(2):223–239

Bignal KL, Ashmore MR, Headley AD, Stewart K, Weigert K (2007) Ecological impacts of air pollution from road transport on local vegetation. Appl Geochem 22(6):1265–1271

Bush SE, Pataki DE, Ehleringer JR (2007) Sources of variation in $\delta^{13}C$ of fossil fuel emissions in Salt Lake City, USA. Appl Geochem 22(4):715–723

Butler TJ, Likens GE, Vermeylen FM, Stunder BJB (2005) The impact of changing nitrogen oxide emissions on wet and dry nitrogen deposition in the northeastern USA. Atmos Environ 39(27):4851–4862

Bytnerowicz A, Sanz MJ, Arbaugh MJ, Padgett PE, Jones DP, Davila A (2005) Passive sampler for monitoring ambient nitric acid (HNO_3) and nitrous acid (HNO_2) concentrations. Atmos Environ 39(14):2655–2660

Cape JN, Tang YS, van Dijk N, Love L, Sutton MA, Palmer SCF (2004) Concentrations of ammonia and nitrogen dioxide at roadside verges, and their contribution to nitrogen deposition. Environ Pollut 132(3):469–478

Casciotti KL, Sigman DM, Hastings MG, Böhlke JK, Hilkert A (2002) Measurement of the oxygen isotopic composition of nitrate in seawater and freshwater using the denitrifier method. Anal Chem 74(19):4905–4912

Clarke JF, Edgerton ES, Martin BE (1997) Dry deposition calculations for the clean air status and trends network. Atmos Environ 31(21):3667–3678

Clark-Thorne ST, Yapp CJ (2003) Stable carbon isotope constraints on mixing and mass balance of CO_2 in an urban atmosphere: Dallas metropolitan area, Texas, USA. Appl Geochem 18(1):75–95

Dawson TE, Mambelli S, Plamboeck AH, Templer PH, Tu KP (2002) Stable isotopes in plant ecology. Annu Rev Ecol Syst 33:507–559

Divers MT, Elliott EM, Bain DJ (2012) Constraining nitrogen inputs to urban streams from leaking sewers using inverse modeling: implications for dissolved inorganic nitrogen (DIN) retention in urban environments. Environ Sci Technol 47(4):1816–1823

Elliott EM, Kendall C, Wankel SD, Burns DA, Boyer EW, Harlin K, Bain DJ, Butler TJ (2007) Nitrogen isotopes as indicators of NO_x source contributions to atmospheric nitrate deposition across the midwestern and northeastern United States. Environ Sci Technol 41(22):7661–7667

Elliott EM, Kendall C, Boyer EW, Burns DA, Lear GG, Golden HE, Harlin K, Bytnerowicz A, Butler TJ, Glatz R (2009) Dual nitrate isotopes in dry deposition: utility for partitioning NOx source contributions to landscape nitrogen deposition. J Geophys Res 114(G4):G04020

Felix JE, Elliott EM (2013) The agricultural history of human–nitrogen interactions as recorded in ice core $\delta15N–NO3$. Geophys Res Lett. doi:10.1002/grl.50209

Felix JD, Elliott EM, Shaw SL (2012) Nitrogen isotopic composition of coal-fired power plant NO_x: influence of emission controls and implications for global emission inventories. Environ Sci Technol 46(6):3528–3535

Garten CTJ (1993) Variation in foliar ^{15}N abundance and the availability of soil nitrogen on Walker Branch Watershed. Ecology 74(7):2098–2113

Gebauer G, Schulze ED (1991) Carbon and nitrogen isotope ratios in different compartments of a healthy and a declining *Picea abies* forest in the Fichtelgebirge, NE Bavaria. Oecologia 87(2):198–207

Gilbert NL, Goldberg MS, Brook JR, Jerrett M (2007) The influence of highway traffic on ambient nitrogen dioxide concentrations beyond the immediate vicinity of highways. Atmos Environ 41(12):2670–2673

Golden HE, Boyer EW, Brown MG, Elliott EM, Lee DK (2008) Simple approaches for measuring dry atmospheric nitrogen deposition to watersheds. Water Resour Res 44:W00D02

Groffman PL, Law NL, Belt KT, Band LE, Fisher GT (2004) Nitrogen fluxes and retention in urban watershed ecosystems. Ecosystems 7:393–403

Hargreaves KJ, Fowler D, Storeton-West RL, Duyzer JH (1992) The exchange of nitric oxide, nitrogen dioxide and ozone between pasture and the atmosphere. Environ Pollut 75(1):53–59

Hastings MG, Sigman DM, Lipschultz F (2003) Isotopic evidence for source changes of nitrate in rain at Bermuda. J Geophys Res 108(D24):4790

Hatt BE, Fletcher TD, Walsh CJ, Taylor SL (2004) The influence of urban density and drainage infrastructure on the concentrations and loads of pollutants in small streams. Environ Manag 34(1):112–124

Hauglustaine DA, Granier C, Brasseur GP, Mégie G (1994) The importance of atmospheric chemistry in the calculation of radiative forcing on the climate system. J Geophys Res 99(D1):1173–1186

Heaton THE (1990) $^{15}N/^{14}N$ ratios of NO_x from vehicle engines and coal-fired power stations. Tellus Ser B 42:304–307

Högberg P (1997) Tansley review No. 95 ^{15}N natural abundance in soil-plant systems. New Phytol 137(2):179–203

Jung K, Gebauer G, Gehre M, Hofmann D, Weißflog L, Schüürmann G (1997) Anthropogenic impacts on natural nitrogen isotope variations in *Pinus sylvestris* stands in an industrially polluted area. Environ Pollut 97(1–2):175–181

Keeling CD (1958) The concentration and isotopic abundances of atmospheric carbon dioxide in rural areas. Geochim et Cosmochim Acta 13(4):322–334

Kirby C, Greig A, Drye T (1998) Temporal and spatial variations in nitrogen dioxide concentrations across an urban landscape: Cambridge, UK. Environ Monit Assess 52(1):65–82

Kirchner M, Jakobi G, Feicht E, Bernhardt M, Fischer A (2005) Elevated NH_3 and NO_2 air concentrations and nitrogen deposition rates in the vicinity of a highway in Southern Bavaria. Atmos Environ 39(25):4531–4542

Li D, Wang X (2008) Nitrogen isotopic signature of soil-released nitric oxide (NO) after fertilizer application. Atmos Environ 42(19):4747–4754

Lichtfouse E, Lichtfouse M, Jaffrézic A (2002) $\delta^{13}C$ values of grasses as a novel indicator of pollution by fossil-fuel-derived greenhouse gas CO_2 in urban areas. Environ Sci Technol 37(1):87–89

Moomaw WR (2002) Energy, industry and nitrogen: strategies for decreasing reactive nitrogen emissions. AMBIO 31(2):184–189

Moore H (1977) The isotopic composition of ammonia, nitrogen dioxide and nitrate in the atmosphere. Atmos Environ 11(12):1239–1243

Neuman JA, Parrish DD, Trainer M, Ryerson TB, Holloway JS, Nowak JB, Swanson A, Flocke F, Roberts JM, Brown SS, Stark H, Sommariva R, Stohl A, Peltier R, Weber R, Wollny AG, Sueper DT, Huber G, Fehsenfeld FC (2006) Reactive nitrogen transport and photochemistry in urban

plumes over the North Atlantic Ocean. J Geophys Res 111(D23):D23S54

Okano K, Machida T, Totsuka T (1988) Absorption of atmospheric NO2 by several herbaceous species: estimation by the 15 N dilution method. New Phytol 109(2):203–210

Padgett PE, Cook H, Bytnerowicz A, Heath RL (2009) Foliar loading and metabolic assimilation of dry deposited nitric acid air pollutants by trees. J Environ Monit 11(1):75–84

Pearson J, Wells DM, Seller KJ, Bennett A, Soares A, Woodall J, Ingrouille MJ (2000) Traffic exposure increases natural ^{15}N and heavy metal concentrations in mosses. New Phytol 147(2):317–326

Pennsylvania_Department_of_Transportation (2009) Traffic volume map of Westmoreland County, PA, vol 9/18

Roadman MJ, Scudlark JR, Meisinger JJ, Ullman WJ (2003) Validation of Ogawa passive samplers for the determination of gaseous ammonia concentrations in agricultural settings. Atmos Environ 37(17):2317–2325

Saurer M, Cherubini P, Ammann M, De Cinti B, Siegwolf R (2004) First detection of nitrogen from NO$_x$ in tree rings: a ^{15}N/^{14}N study near a motorway. Atmos Environ 38(18):2779–2787

Sigman DM, Casciotti KL, Andreani M, Barford C, Galanter M, Böhlke JK (2001) A bacterial method for the nitrogen isotopic analysis of nitrate in seawater and freshwater. Anal Chem 73(17):4145–4153

Singer BC, Hodgson AT, Hotchi T, Kim JJ (2004) Passive measurement of nitrogen oxides to assess traffic-related pollutant exposure for the East Bay Children's Respiratory Health Study. Atmos Environ 38(3):393–403

Tang YS, Cape JN, Sutton MA (2001) Development and types of passive samplers for monitoring atmospheric NO$_2$ and NH$_3$ concentrations. Sci World J 1:513–529

Thoene B, SchrÖDer P, Papen H, Egger A, Rennenberg H (1991) Absorption of atmospheric NO$_2$ by spruce (Picea abies L. Karst.) trees. New Phytol 117(4):575–585

U.S._EPA_CASTNET (2008) Trends in wet and dry N deposition at LRL117 (Laurel Hill), vol 9/18

Wellburn A (1990) Tansley review No. 24 why are atmospheric oxides of nitrogen usually phytotoxic and not alternative fertilizers? New Phytol 115(3):395–429

Yu CH, Morandi MT, Weisel CP (2008) Passive dosimeters for nitrogen dioxide in personal/indoor air sampling: a review. J Expo Sci Environ Epidemiol 18(5):441–451